Enhancing the surge margin of a Centrifugal Compressor with different Blade Tip Geometry

Ibrahim Shahin

Mechanical Engineering Department, Shoubra faculty of Engineering, Benha University, Egypt

Abstract— *The reliability operation for small fuel cells and hybrid fuel cell with gas turbine requires centrifugal compressor surge prevention. This study concerns a high speed centrifugal compressor stage with different blade tip geometries. The investigations were performed with unsteady three-dimensional, compressible flow simulations. A novel parameterization method has been developed to alter the tip geometry of an impeller blade. Different tip geometries are investigated includes flat tip blade, main blade winglet, main and splitter blade winglet and finally pressure side grooved tip. The performance and internal flow results are presented at surge, design and near choke points. The conclusion is that the tip geometry has a significant effect on the compressor performance and the operation stability at lower flow rates. The pressure ratio and surge margin for the blades with winglet have been improved, and decreased for the grooved tip geometry. More uniform flow at impeller outlet with winglet blade. The use of winglet tip displaces the tip leakage vortex away from the blade and weakening the impingement effect. The winglet tip reduces the aerodynamic losses by unloading the tip section, reducing the leakage flow rate and turning the leakage flow in a more stream wise direction.*

Keywords— Blade Tip; Centrifugal Compressor; Performance and Stability.

I. INTRODUCTION

Centrifugal compressors are used in a wide variety of engineering applications for power generation and fuel cell is one of them. Fuel cell takes advantage of the electro-chemical reaction between oxygen and hydrogen to produce electricity. The compressor performance and stability has a big effect on the operation of the fuel cell. The solid oxide fuel cell (SOFC) integrated with a gas turbine (GT) has a potential for high efficiency electricity production with low environmental emissions. However, SOFC/GT hybrid systems face many challenges when it comes to load change and part-load operation. A gas turbine alone has good dynamic properties, but part-load performance can be rather poor. At any operation point, compressor surge must be prevented. Tip leakage flow is important for high speed transonic centrifugal compressor. The

tip leakage flow has serious effect on the performance and stable operation. The effect is much more deleterious in centrifugal compressors than axial compressors because a centrifugal compressor has a long narrow flow passage so that the tip clearance occupies a large portion of the flow passage.

Tip leakage flow in centrifugal compressor has been studied by many researchers, and its effect on the performance reduction is also investigated. The experimental and numerical studies of (Lakshminarayana, [1]; Moor et al., [2]; Farge et al., [3]; Hah, [4]; Larosiliere et al., [5]; Myong and Yang, [6]) indicated that the leakage flow changes the behavior of secondary flow and the location of low momentum flow regions. The losses due to tip leakage flow reach 20-40% of the total losses. In fact, a review of the published work on tip leakage flow control reveals that centrifugal compressors and more generally radial machines have received much less attention than their axial counterparts in these areas, independently of the domain of application. The role played by tip leakage and blade tip geometry in axial turbomachines has received much attention, including axial compressors, turbines and fans. The experimental measurements by Inoue et al. [7] show that the tip clearance has a big effect on the tip leakage flow characteristics. Furukawa and Inoue et al. [8] also studied the tip leakage vortex separation in axial flow compressor. The results indicated that a significant improve in the aerodynamic performance is resulted due to reducing the tip leakage mass flow rate.

Fujita et al. [9] and Moore et al. [10] investigated the effect of stationary casing treatment for axial compressors. The tip leakage flow is reduced with casing treatments. Pak et al. [11] performed detailed measurements on the complex flow field due to tip flow. Farge et al. [12], Ishida et al. [13] investigated the relative interaction between leakage flow, shock wave and boundary layer in a centrifugal compressor. The research performed by Barton et al. [14], Ishida et al. [15], and Dickmann et al. [16] indicated that the casing treatment methods affect the performance of centrifugal compressor. The present paper describes a study of the aerodynamic aspects of tip leakage flow in a centrifugal compressor with shroud less impeller. A numerical optimization process of different tip

geometry is described. The way in which the geometry was parameterized and the way in which the optimization process was carried out was designed to reach several goals. The first goal was to gain more insight into the effect of the winglet on the flow physics and performance. The second was to investigate the trade-offs between the tip geometry effect on performance and its effect on the stable working rang of the centrifugal compressor. Tip leakage flow results in a considerable amount of aerodynamic loss in impeller flow field as discussed in the above section for the impeller with flat tip. One way of reducing tip losses is to use proper tip treatments. The specific tip treatments subject to investigation in this paper include special extensions of rotor tip winglet and tip grooves.

II. NUMERICAL METHOD

2.1 Computational model

NASA CC3 vanless diffuser radial compressor is examined by [17-20]. The numerical model divided into three parts; straight pipe inlet domain, semi open rotor and diffuser equipped with impeller back flow region. The hub cavity flow is directed to labyrinth shaft seal. The inlet domain is extended for length equal to 5 times the compressor intake diameter, to ensure that the flow reaches the fully develop condition. The impeller out flow is directed to a vanless diffuser with an annular radial-to-axial bend. To avoid the effect of the outlet boundary conditions on the simulated flow inside the compressor parts, compressor exit is extended in the axial direction. The hub side cavity and shaft labyrinth seal are also modeled. Fig.1 presents the domain geometry included in the present model.
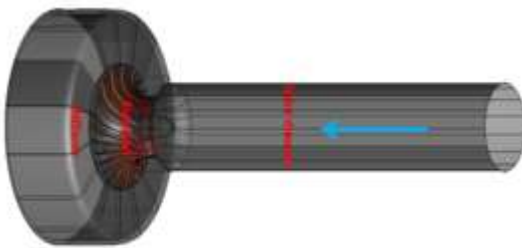

Fig.1: Computational domain and Flow path in the compressor stage.

2.2 Numerical Model Meshes

The ICEM CFD [21] blocking tool has been used to develop the model mesh, which has hexahedral element type; the computational grid generated is shown in Fig.2. To ensure the ability of the present model to capture the boundary layers, the grid is concentrated near the walls boundaries and elements are enlarged by 5% as moved away from it. Sufficient number of elements has been used in the tip flow clearance to capture the effect of tip leakage flow. Careful check for grid independence was also conducted; three numbers of computational nodes were checked and 3.23 million of nodes were used as no change

in results with increasing the mesh nodes higher that number [23]. The numbers of nodes are changed by increasing the number of elements for the impeller and diffuser in meridional, radial and spanwise directions.
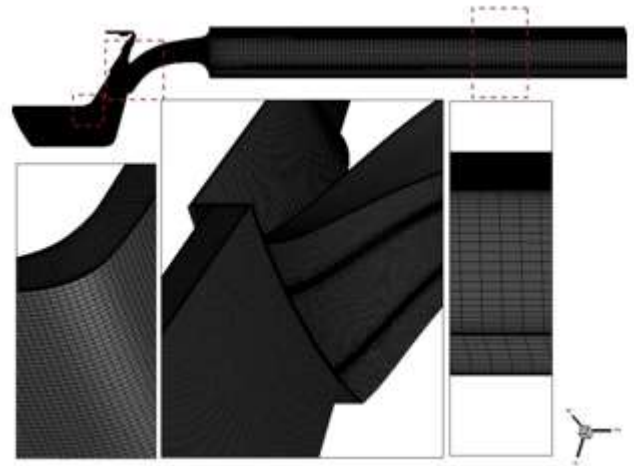

Fig.2: Hexahedral meshes for the numerical domain.

2.3 Solver

The compressible, three-dimensional, Unsteady Reynolds-Averaged Navier-Stokes URANS equations are solved. All the numerical calculations were performed using FLUENT [21]. A compressible, density based solver with SIMPLEC method for pressure-velocity coupling. The solved equations were discretized with second order of scheme. To capture the impeller rotation and the interaction between the rotating and stationary parts, the sliding mesh is assigned for the impeller fluid domain. The interface boundary conditions are used to connect the moving and stationary cell zones. The relative position between moving and stationary domains is updated with time [21]. The sliding mesh technique is computationally expensive when compared with moving reference frame techniques. But the rotating is rotating relative to the stationary fluid domain. Also, the blade passage effects are well captured and the position of the impeller relative to the diffuser is captured, by which the relevant fluctuations are resolved.

The turbulence is simulated by Renormalized Navier Stokes K-ε RNG turbulence model with non-equilibrium near wall treatments, with 2% turbulence intensity at flow inlet. In K- ε turbulent models, an equation for kinetic energy k is applied to find out the eddy viscosity. The transport equations for k and ε

$(=(\mu/\rho)\,\overline{(\partial u_i^{'}/\partial x_j)^2}\,)$ as dissipation rate of k are indicated by Eq.1, 2 and 3.

$$\rho\frac{\partial k}{\partial t} + \rho\overline{U}_j\frac{\partial k}{\partial x_j} = \frac{\partial}{\partial x_j}\left[\left(\mu + \frac{\mu_t}{\sigma_k}\right)\frac{\partial k}{\partial x_j}\right] + P_k - \rho\varepsilon \quad (1)$$

$$\rho\frac{\partial\varepsilon}{\partial t} + \rho\overline{U}_j\frac{\partial\varepsilon}{\partial x_j} = \frac{\partial}{\partial x_j}\left[\left(\mu + \frac{\mu_t}{\sigma_\varepsilon}\right)\frac{\partial\varepsilon}{\partial x_j}\right] + C_1 P_k\frac{\varepsilon}{k} - C_2\rho\frac{\varepsilon^2}{k}$$

(2)

$$P_k = -\rho\overline{u_i' u_j'}\frac{\partial\overline{U_i}}{\partial x_j}$$ (3)

The constants are empirically found for attached boundary layer flow as $\sigma_k = 1$, $\sigma_\varepsilon = 1.3$, $C_1 = 1.44$ and $C_2 = 1.92$ but they are not general and have to be found for other problems. (White et al, 1991). Once k and ε are obtained, the turbulent eddy viscosity is modelled as $\mu_t = C_\mu\rho\frac{k^2}{\varepsilon}$ with $C_\mu = 0.09$ and, then, mean momentum equation can be solved.

Indeed, for wall treatment, some semi-empirical functions (*wall function*) are set to link velocity and turbulent parameters at the wall to the corresponding variables at the cells close to the wall. The wall functions save the computational time because the grid does not resolve the region just above the wall and it is modelled with wall functions. The temporal discretization is of second order scheme. For discretization in space, a second order accuracy was used. The simulation was conducted on a server with 4 AMD Opteron processor, 48 cores and 128 GB of RAM. To resolve the complicated unsteady flow phenomena in centrifugal compressor, fin grid resolution have been used very small time step and small Courant number with values smaller than unity to be consistent with the flow properties which, for this case, gives a time step of 6.674e-6.

2.4 Boundary Conditions

The computational domain is consisting 24° sector to cover only one blade passage Fig. 2 and rotational periodic boundary condition was used to save the calculation time. The casing walls and blade surfaces were simulated with no slip wall boundary condition. To specify the operating point for the compressor, the mass flow boundary condition is identified at the inlet. The atmospheric pressure is used for the inlet air and temperature equals to 288k. The sliding mesh used to simulate the impeller rotation, requires the use of interface boundary condition at inlet and outlet of each fluid domain. The pressure outlet boundary condition is specified at the compressor outlet and at the seal exit which equal to atmospheric pressure.

2.5 Convergence Criteria

To ensure the solution convergence, the residuals of the governing equations decreased by three orders of magnitude. Also, the calculations were not stopped until the residuals reached a stable value. In addition, the mass flow rate and static

pressure at inlet and outlet were monitored to make sure that it reached a stable value. The numerical model used in this study has been validated in author works [22 to 24].

2.6 Tip Treatment Geometries

The investigated tip geometries included in this paper are flat blade tip, winglet for main blades, winglet for main and splitter blades and blades with pressure side grooved tip. The tip geometry and mesh are shown in Fig.3 and Fig. 4 respectively.
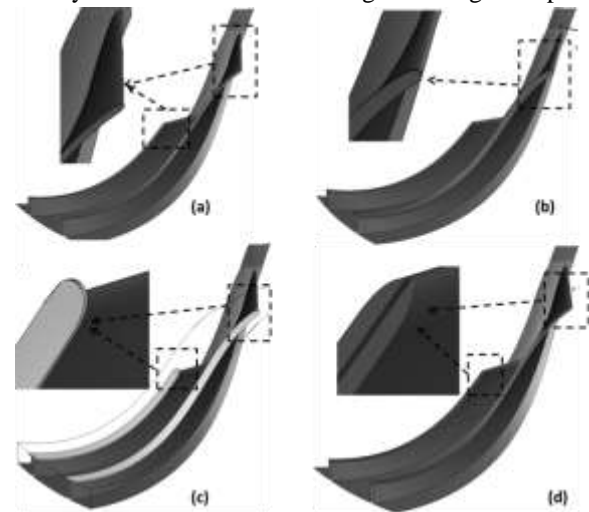

Fig.3: Studied tip geometries: (a) Flat blade tip, (b) Winglet for main blades, (c) Winglet for main and splitter blades, and (d) Blades with pressure side grooved tip.
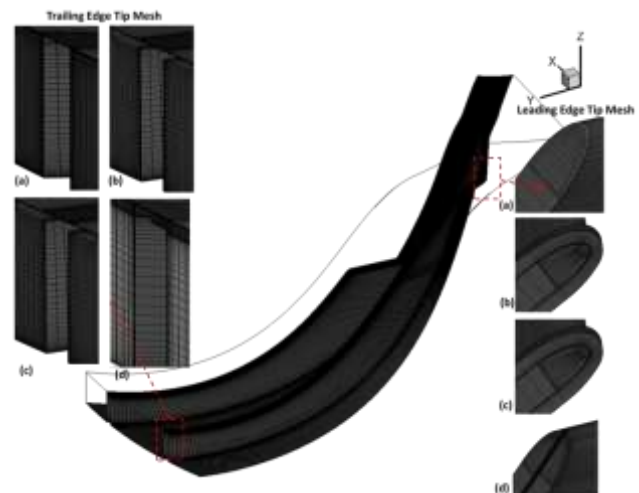

Fig.4: Studied cases mesh: (a) Flat blade tip, (b) Winglet for main blades, (c) Winglet for main and splitter blades, and (d) Blades with pressure side grooved tip.

III.   RESULTS AND DISCUSSION

The pressure ratio variation with mass flow rate is shown in Fig.5 for different tip blade geometries and compared with the

base case with flat tip geometry. It can be seen that the pressure ratio for the cases with new tips has been increased except for the case with grooved blade tip. The surge inception mass flow rate is also decreased for the cases with using winglet, but slightly increased for case with grooved tip. The surge margin for winglet tip cases has been improved due to the control of the tip vortex and higher stable mass flow due to the reduction of the tip mass flow rates. The choke flow limit is noticed to be decreased resulting from the area reduction due to the use of winglet. On the other hand, choke limit is slightly increased for grooved tip case. The pressure side grooved tip causes an increase for the flow area and an increase for tip leakage flow.
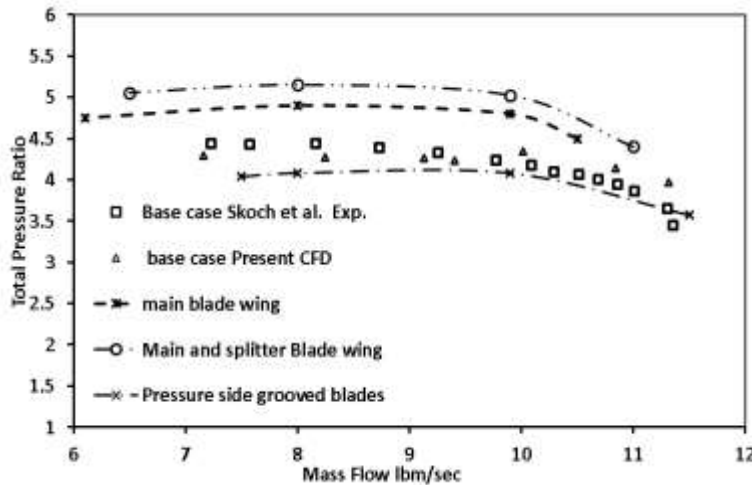

Fig.5: Pressure ratios with mass flow rate for compressor with different tip geometries.

To validate the pressure developed inside the impeller, the present CFD flow velocity is compared with Larosiliere et al. [25]. Figure 6 shows the static pressure rise along the shroud for the present CFD results and experimental results of Larosiliere et al. [25]. The area averaged static pressure from the present CFD agree well with the measurements till 30% of the chord length, after that the static pressure is slightly under estimated. This difference is due to the constant tip clearance used in Larosiliere et al. [25].
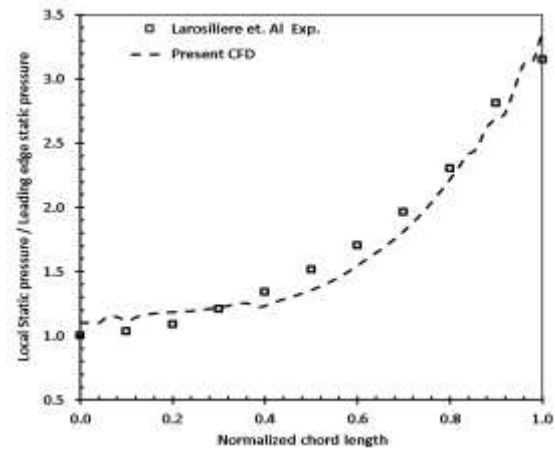

Fig.6: Average static pressure distributions along the shroud for (a) Measured results of Lavoisier et al. [25], (b) present CFD results.

In order to justify the improvement in the compressor pressure ratio, the developed pressure is averaged through the impeller and diffuser stream wise pass. Fig.7 shows the pressure along the compressor stage for different tip geometries, the horizontal axis represents the normalized length through the stream wise direction, point 0 represents the impeller inlet, point 1 represents the impeller outlet, point 1.4 represents the diffuser bend and diffuser outlet is represented by point 2. The developed pressure through the impeller is enhanced when using winglet, with higher enhancement for the case with winglet at the main blade. The use of winglet on main and splitter blades also enhance the pressure ratio, but an increase on the flow velocity results from the reduction in the flow area, which will increase the friction losses through the impeller.Fig.8 presents the developed pressure for the case with main blade winglet at off design conditions. The pressure at the inducer area is decreased when compared with the case with flat tip, resulting from the increase of the velocity due to the reduction on the flow area.
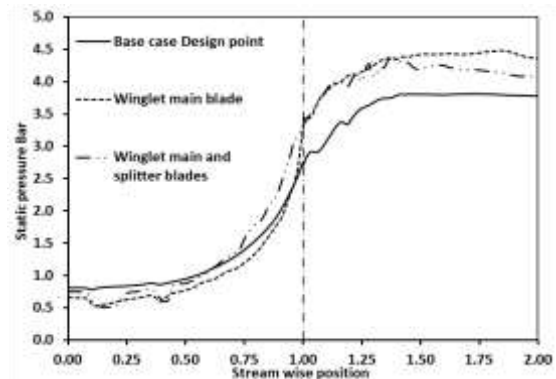

Fig.7: Developed static pressure through the compressor stage for different tip geometries at design flow rate.
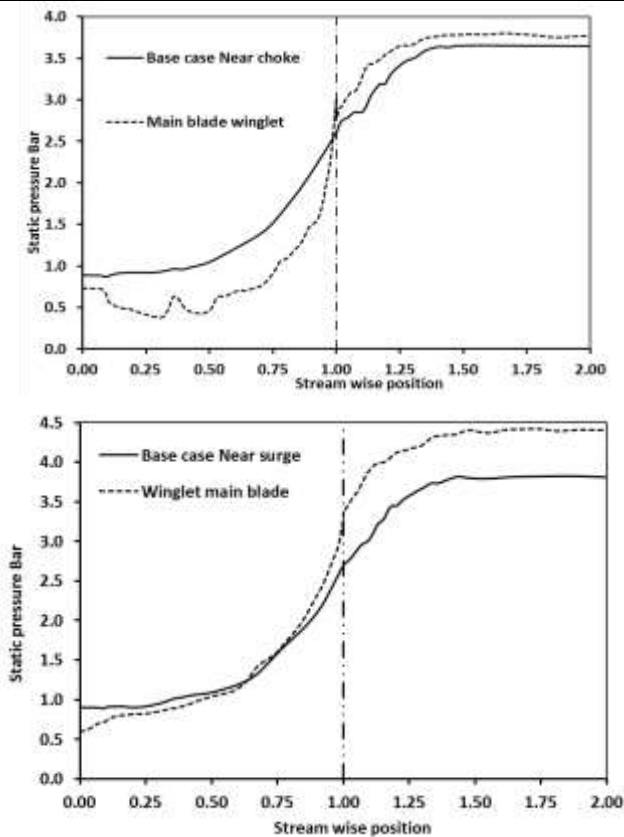
Fig.8: Developed static pressure through the compressor stage at off design condition.

The radial velocity normalized by the impeller tip speed distribution is shown in Fig.9 at the impeller outlet. The jet-wake flow structure is observed for all three-operating point, which characterized by low radial and high tangential velocities near the blade suction side. The trend for the radial velocity is reversed near the blade pressure side, high radial velocity and low tangential velocity components are observed. Low radial velocity component characterizes the blade wake region that observed near the impeller hub. The jet pattern is found near the blade pressure side, while the wake pattern has been observed near the suction side with higher tangential velocity component. As the operating point is moved close to the surge, tangential velocity component is increased at the mid-span and near the blades suction side. The jet appears as a region of low tangential velocities in the pressure side hub corner. The tip leakage flow results in a low negative radial velocity region close to the impeller shroud especially at the lower flow rates, at which the blade wake and the jet interact strongly and interchange momentum. The near surge operating point is also characterized by a stagnant or back flow near the impeller shroud.

Fig.10 shows the radial velocity at impeller outlet for different tip geometries. Low momentum flow region caused by reversed secondary flow was observed at the blade suction side near the corner of impeller casing. When using winglet for the main or splitter blades, the velocity distribution at the impeller outlet is improved to be more uniform and the low momentum reverse flow region is disappeared and the effect of jet wake flow structure is decreased. The pressure ratio of both impellers with winglets higher than that of the impeller with flat tip, the reason for the pressure ratio improvement is that the reduction of the loss in the vanless diffuser parts due to a more uniform distribution of the velocity at the impeller outlet. The uniform velocity distribution near the corner of the impeller casing wall and the blade suction surface in the impeller with winglet tip is higher than that in the impeller with flat tip. The mass flow at impeller inlet is shown in Fig.11 with the flow time, when working at surge flow rate. The base case with flat tip has the highest mass fluctuation with negative values, which indicate the surge event existence. The stability is improved for cases with winglet tips, and lowest fluctuations are detected for case with winglet tip for main and splitter blades.
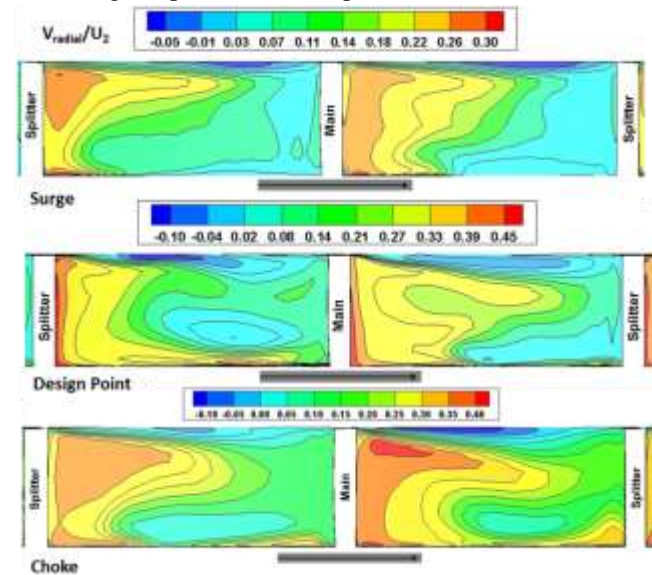

Fig.9: Shows a comparison of the radial velocity distributions normalized by the impeller tip speed at the impeller outlet.
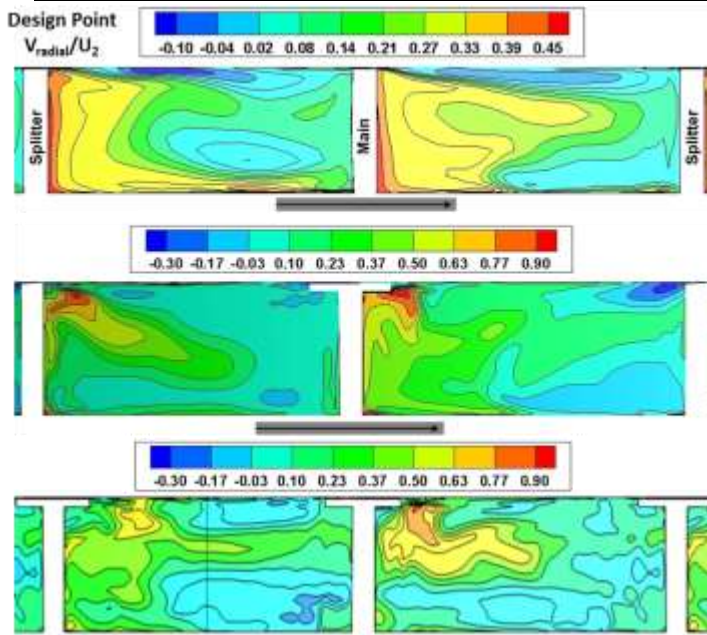
Fig.10: Effect tip geometry on the radial velocity at impeller outlet for different tips.
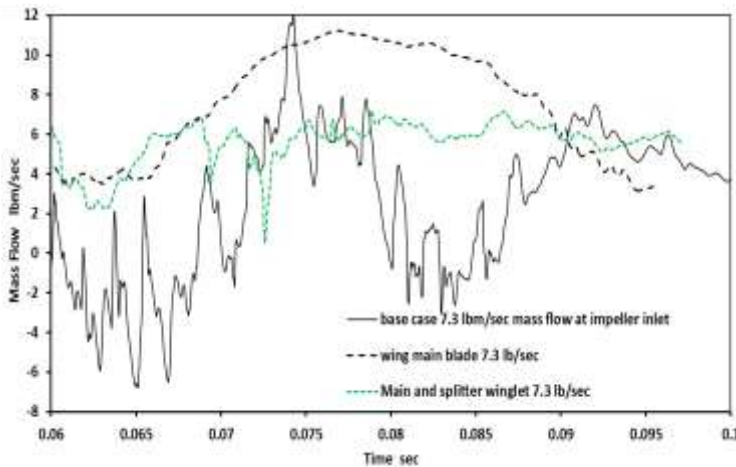

Fig.11: Effect tip geometry on the impeller inlet mass flow stability at surge.

IV.   CONCLUSIONS

The three dimensional URANS CFD simulation has been developed for high speed centrifugal compressor with a vanless diffuser. Different blade tips have been tested to improve the compressor performance and stability working range at lower flow rates. The flat blade tip, winglet main blade tip, winglet main and splitter tip and pressure side groove tips were studied numerically at different operating flow rates. The performance curves for the studied cases are presented and discussed. The average developed pressure through the impeller and diffuser were analyzed for all studied cases and different operating flow rates. The main results obtained and the phenomena described in this paper indicates an improvement for the pressure ratio

with winglet tip cases, while a noticed decrease in the developed pressure ratio with the use of grooved tip due to the increase of tip leakage flow. The base case with flat tip has the highest mass fluctuation with negative values, which indicate the surge event existence. The stability at lower flow rates is improved for cases with winglet tips, and lowest fluctuations are detected for case with winglet tip for main and splitter blades.

REFERENCES

[1] Lakshminarayana, B., 1970, "Methods of Predicting the Tip Clearance Effects in Axial Flow Turbomachines," Journal of Basic Engineering, Vol. 92, pp. 467--482.

[2] Moore, J., Moore, J.G. and Timmis, P.H., 1984, "Performance Evaluation of Centrifugal Compressor Impellers Using Three-Dimensional Viscous Flow Calculations," Journal of Engineering for Gas Turbines and Power, Vol. 106, pp. 475~481.

[3] Farge, T.Z., Johnson, M.W. and Maksoud, T. M. A., 1989, "Tip Leakage in a Centrifugal Impeller," Journal of Turbomachinery, Vol. 111, pp. 224- 249.

[4] Hah, C.A., 1986, "A Numerical Modeling of Endwall and Tip-Clearance Flow of an Isolated Compressor Rotor," Journal of Engineering for Gas Turbines and Power, Vol. 108, pp. 15--21.

[5] Larosiliere, L.M., Skoch, G.J. and Prahst, P.S., 1999, "Tip Leakage in a Centrifugal Impeller Using Computational Fluid Dynamics and Measurements," Journal of Propulsion and Power, Vol. 15, No. 5, pp. 623--632.

[6] Myong, H. K. and Yang, S. Y., 2003, "Numerical Study on Flow Characteristics at Blade Passage and Tip Clearance in a Linear Cascade of High Performance Turbine Blade," KSME international Journal, Vol. 17, No. 4, pp. 606--616.

[7] Inoue, M., Kuroumaru, M. and Fukuhara, M., 1986. Behavior of tip leakage flow behind an axial compressor rotor. Journal of Engineering for Gas Turbines and Power, 108(1), pp.7-14.

[8] Furukawa, M., Inoue, M., Saiki, K. and Yamada, K., 1998, June. The role of tip leakage vortex breakdown in compressor rotor aerodynamics. In ASME 1998 International Gas Turbine and Aero-engine Congress and Exhibition (pp. V001T01A054-V001T01A054). American Society of Mechanical Engineers.

[9] Fujita, H. and TAKATA, H., 1984. A study on configurations of casing treatment for axial flow compressors. Bulletin of JSME, 27(230), pp.1675-1681.

[10] Moore, R. D., Kovich, G., and Blade, R. J., 1971, "Effect of Casing Treatment on Overall and Blade-Element

Performance of a Compressor Rotor," NASA, Tech. Rep. TN-D6538.

[11] Pak, H., Krain, H. and Hoffmann, B., 1994, March. Flow field analysis in a high-pressure ratio centrifugal compressor. In in AGARD, Technology Requirements for Small Gas Turbines 12 p (SEE N94-34431 10-07) (Vol. 1).

[12] Farge, T.Z., Johnson, M.W. and Maksoud, T.M.A., 1989. Tip leakage in a centrifugal impeller. Journal of Turbomachinery, 111(3), pp.244-249.

[13] Ishida, M., Ueki, H. and Senoo, Y., 1990. Effect of blade tip configuration on tip clearance loss of a centrifugal impeller. Journal of Turbomachinery, 112(1), pp.14-18.

[14] Barton, M.T., Mansour, M.L., Liu, J.S. and Palmer, D.L., 2006. Numerical optimization of a vaned shroud design for increased operability margin in modern centrifugal compressors. Journal of turbomachinery, 128(4), pp.627-631.

[15] Ishida, M., Sakaguchi, D. and Ueki, H., 2005, January. Optimization of inlet ring groove arrangement for suppression of unstable flow in a centrifugal impeller. In ASME Turbo Expo 2005: Power for Land, Sea, and Air (pp. 841-850). American Society of Mechanical Engineers.

[16] Dickmann, H.P., Wimmel, T.S., Szwedowicz, J., Filsinger, D. and Roduner, C.H., 2005, January. Unsteady flow in a turbocharger centrifugal compressor: 3D-CFD-simulation and numerical and experimental analysis of impeller blade vibration. In ASME Turbo Expo 2005: Power for Land, Sea, and Air (pp. 1309-1321). American Society of Mechanical Engineers.

[17] Mckain, T.F. And Holbrook, G.J., 1997, "Coordinates for a high performance 4:1 pressure ratio centrifugal compressor" Lewis Research Center, NASA-23268.

[18] Skoch, G.J., Prahst, P.S., Wernet, M.P. and Strazisar, A.J., 1997, "Laser Anemometer Measurements of the Flow Field in a 4:1 Pressure Ratio Centrifugal Impeller" Proceedings of ASME Turbo-Expo 97, Orlando, Florida.

[19] Wernet, M.P., Bright, M.M. and Skoch, G.J., 2002, "An Investigation of Surge in a High-Speed Centrifugal Compressor Using Digital PIV "NASA/TM—2002-211832.

[20] Ni, R.H. and Fan, G. ,2009, " CFD Simulation of a High-Speed Centrifugal Compressor Using Code Leo and Code Wand" Technical report, ADS Aerodynamic Solutions, Inc.

[21] ANSYS FLUENT Theory guide, November 2010.

[22] Shahin, I., Gadala, M., Alqaradawi, M., & Badr, O. (2014, June). Unsteady CFD Simulation for High Speed Centrifugal Compressor Operating Near Surge. In ASME Turbo Expo 2014: Turbine Technical Conference and Exposition (pp. V02DT44A045-V02DT44A045). American Society of Mechanical Engineers.

[23] Shahin, I., Gadala, M., Alqaradawi, M., & Badr, O. (2015). Large Eddy Simulation for a Deep Surge Cycle in a High-Speed Centrifugal Compressor with Vaned Diffuser. Journal of Turbomachinery, 137(10), 101007.

[24] Halawa, T., Alqaradawi, M., Gadala, M. S., Shahin, I., & Badr, O. (2015). Numerical investigation of rotating stall in centrifugal compressor with vaned and vaneless diffuser. Journal of Thermal Science, 24(4), 323-333.

[25] Larosiliere, L. M., Skoch, G. J., & Prahst, P. S. (1997). Aerodynamic synthesis of a centrifugal impeller using CFD and measurements. National Aeronautics and Space Administration.